Title	Microdroplet formation of water and nanofluids in heat-induced microfluidic T-junction
Author(s)	Murshed, S. M. Sohel; Tan, Say-Hwa; Nguyen, Nam-Trung; Wong, Teck Neng; Yobas, Levent
Citation	Murshed, S. M. S., Tan, S. H., Nguyen, N. T., Wong, T. N., & Yobas, L. (2009). Microdroplet formation of water and nanofluids in heat-induced microfluidic T-junction. Microfluidics and Nanofluidics, 6(2), 253-259.
Date	2009
URL	http://hdl.handle.net/10220/7874
Rights	© Springer-Verlag 2008. This is the author created version of a work that has been peer reviewed and accepted for publication by Microfluidics and Nanofluidics, Springer-Verlag. It incorporates referee's comments but changes resulting from the publishing process, such as copyediting, structural formatting, may not be reflected in this document. The published version is available at: DOI: [http://dx.doi.org/10.1007/s10404-008-0323-3].

Microdroplet formation of water and nanofluids in heat-induced microfluidic T-junction

S. M. Sohel Murshed[1] · Say Hwa Tan[1] ·Nam Trung Nguyen[1,*] · Teck Neng Wong[1] · Levent Yobas[2]

[1]School of Mechanical and Aerospace Engineering, Nanyang Technological University, 50 Nanyang Avenue, Singapore 639798, Singapore

[2]Institute of Microelectronics, Science Park II, Singapore 117685l, Singapore

Abstract This paper reports experimental investigations on the droplet formation and size manipulation of deionized water and nanofluids in a microfluidic T-junction at different temperatures. Investigations of the effect of microchannel depths on the droplet formation process showed that the smaller the depth of the channel the larger the increase of droplet size with temperature. Sample nanofluids were prepared by dispersing 0.1 volume % of titanium dioxide (TiO_2) nanoparticles of 15 nm and 10×40 nm in deionized water for their droplet formation experiments. The heater temperature also affects the droplet formation process. Present results demonstrate that nanofluids exhibit different characteristics in droplet formation with the temperature. Addition of spherical-shaped TiO_2 (15 nm) nanoparticles in deionized water results in much smaller droplet size compared to the cylindrical-shaped TiO_2 (10×40) nm) nanoparticles. Besides changing the interfacial properties of based fluid, nanoparticles can influence the droplet formation of nanofluids by introducing interfacial slip at the interface. Other than nanofluid with cylindrical-shaped nanoparticles, the droplet size was found to increase with increasing temperature.

Keywords Microdroplet · Nanofluids · Nanoparticle · T-junction · Microchannel

[*]e-mail: mntnguyen@ntu.edu.sg

1 Introduction

Because of the potential applications of droplet-based microfluidics in various important fields such as chemical or biochemical analysis, high throughput screening, and fabrication of microparticles, the formation and manipulation of microdroplets is receiving increased interest from researchers worldwide (Joanicot and Ajdari 2005; Song et al. 2006; Whitesides 2006; Christopher and Anna 2007). Although droplet-based microfluidics is still in its early development stage (Whitesides 2006), applications such as reaction platforms for protein crystallization (Zheng et al. 2003), cell encapsulation (He et al. 2005), polymerase chain reaction (PCR) (Guttenberg et al. 2005) and DNA analysis (Burns et al. 1998) have been reported. Several research efforts have been made on droplet formation devices and techniques, particularly droplet patterns variation in microchannels. For example, the flow focusing device has been used to form small-sized droplets by simply increasing the flow rate of the carrier fluid (Ong et al. 2007) or introducing heating effect (Nguyen et al. 2007). Geometrical techniques have been used to create droplets of various sizes and size distributions (Link et al. 2004). In microfluidics, T-junction microchannel is one of the most frequently used configurations for droplet formation and manipulation (Thorsen et al. 2007; Nisisako et al. 2002; Xu et al.2006). The wide usage of this T-junction geometry is due to the ease of droplet formation and uniformity of the formed droplets. Thorsen et al. (2007) used pressure-controlled flow in a T-junction microchannel to generate water droplets using different types of oils. They reported that the droplet size increases with increasing dispersed phase pressure. Whereas Nisisako et al. (2002) showed a decreased in droplet size with increasing flow rate of the continuous phase. The droplet formation at a T- junction microchannel through shear force between two immiscible fluids can be controlled by various ways such as fluids' flow rates, viscosities, the interfacial

tensions as well as the channel geometry (Link et al. 2004; Schröder et al. 1998; Van der Graaf et al. 2006; Nguyen et al. 2006). Thermally mediated droplets breakup in microchannels was also reported in the literature (Ting et al. 2006).

In droplet-based microfluidics, water is most commonly used as the aqueous phase (also called dispersed phase) to generate droplets through various droplet formation devices such as T-junction microchannel and flow focusing device. On the other side, nanofluid is a new and innovative class of fluids, which is engineered by dispersing nanometer-sized particles in conventional fluids such as deionized water. From the investigations in the past decade nanofluids were found to exhibit different thermophysical and interfacial properties such as thermal conductivity, viscosity, and surface tension as compared to their base fluids (Lee et al. 1999; Murshed et al. 2005; Li and Peterson 2006; Murshed et al. 2008). Apart from the enhanced thermophysical and interfacial properties of nanofluid, this fluid is suitable for use in microfluidics because they contain nanoparticles, which are orders of magnitude smaller than the microfluidic devices themselves. Although the research fields of droplet-based microfluidics (Christopher and Anna 2007) and nanofluids (Murshed et al. 2008a) have attracted great interest of from both communities, no effort has been made to study the use of nanofluids in droplet-based microfluidics.

In this study, we experimentally investigate the formation and manipulation of droplets of deionized water and deionized water-based nanofluids in T-junction microchannel at different temperatures. The effects of microchannel depth and dispersed nanoparticles on the droplet formation process are also studied.

2 Experimental details

Droplets in microchannels are usually generated by two configurations, which are T-junction and flow focusing through a small orifice. Usually, the design of the microchannel is simple and no electrical component is integrated. In this study, two microfluidic T-junction devices with integrated microheater and temperature sensor were designed and fabricated for conducting experiments on temperature dependence of droplet formation and size manipulation.

2.1 Design and fabrication process

The T-junction devices were fabricated using micromachining of glass and polydimethylsiloxane (PDMS). One of the advantages of using PDMS is its better surface finishing as compared to laser machined polymethyl-methacrylate (PMMA) devices (Nguyen et al. 2006; Ting et al. 2006). A low cost transparency mask is used together with lithography process to create the pattern on the glass wafer. After development, titanium layer of 500 Å thickness and platinum layer of 1000 Å thickness are deposited on the glass wafer. Titanium is used as the adhesion layer between glass and platinum while platinum layer acts as heater and temperature sensor. Thereafter, a lift-off process is used to remove the excess metal and the glass micro heater and sensor is ready for use. The microchannel network was fabricated in PDMS using soft lithography. The master mold was fabricated by photo lithography of the thick-film resist SU-8 using a transparency mask. The glass wafer with the patterned microheater and microsensor was subsequently coated with a thin PDMS layer before being bonded to the PDMS part containing the microfluidic network. This step makes sure that all channel walls have the same properties. Bonding is achieved using oxygen plasma treatment on both PDMS surfaces. The alignment was performed manually after the oxygen plasma treatment. The widths of the carrier channel and the

injection channel of both T-junction devices are 100 μm and 50 μm, respectively whereas the depths of channels of two devices are 300 μm and 30 μm. While the sensor detects the temperature at the microchannels, the microheater provides localized heating. The area of the fabricated microdevices measure 1×1 cm^2. Schematic of the T-junction is shown in Fig. 1.

2.2 Experimental setup and procedure

In order to form droplets at the T-junction, two precision syringe pumps (KD Scientific Inc., USA) were used to drive the oil and the aqueous fluids. The flow rates of both the carrier fluid and aqueous fluids were adjusted to form uniform droplets. The temperature sensor was calibrated before the experiments so that its resistance values can be used for *in-situ* temperature measurement. The temperature was adjusted by changing the voltage of the heater and was monitored through the resistance of the sensor. An epi-fluorescent inverted microscope with a filter set (Nikon B-2A) was used to observe the droplets. A sensitive CMOS camera (Basler A504K, Basler AG, Germany), which has a maximum resolution of 1.3 Megapixels and a maximum frame rate of 500 fps, was employed for recording the droplet images. The recorded droplet images were then processed by a customized MATLAB program to obtain the droplet diameter. Since the measured droplet diameter is larger then the channel height, the droplets have the form of a disc. Based on a recent correlation by Nie et al. (2008), the equivalent diameter of a spherical droplet with the same volume can be determined from

$$D_{eq} = 2\{\frac{1}{16}[2D^3 - (D-h)^2(2D+h)]\}^{1/3} \quad (1)$$

where h is the depth of the channel (i.e. 300 μm and 30 μm) and D is the measured diameter of the disk. In this study, the equivalent droplet diameters are determined using Eq. 1.

2.3 Sample preparation and characterization

In this study, two types of sample nanofluids were prepared by dispersing 0.1 volume percentage of titanium dioxide (TiO_2) nanoparticles of 15 nm (spherical-shaped and anatase type) and 10×40 nm (cylindrical-shaped and rutile) in deionized water. While mineral oil (Sigma 5904, Sigma-Aldrich, Singapore) with 2% w/w Span 80 surfactant (Sigma S6760) was used as the carrier fluid in microchannel, deionized water (DIW) and nanofluids with 0.05% w/w fluorescence dye (Sigma F6377) were used as the aqueous fluids for the droplet formation.

Since viscosity and interfacial tension are important parameters in droplet formation and manipulation, the temperature dependence of these properties of carrier fluid and aqueous fluids are characterized. The interfacial tension of the aqueous fluids was measured with a tensiometer system (FTA 200, First Ten Angstroms, USA), while viscosity was measured with a low-shear rheometer (LS 40, Mettler Toledo, Switzerland) at different temperatures. The experimental facilities were calibrated by measuring these properties of deionized water.

3 Results and discussion

3.1 Temperature dependence of viscosity and interfacial tension

The normalized viscosity and interfacial tensions of carrier fluid and aqueous fluids as a function of temperature are presented in Fig. 2. These properties are normalized by their nominal values at 25°C i.e. $\eta^* = \eta(T)/\eta(T = 25^0 C)$ and $\gamma^* = \gamma(T)/\gamma(T = 25^0 C)$. While viscosities of mineral oil with 2 w/w % surfactant (Span 80) and nanofluid at 25°C are 26.4 mPa.s and 0.93 mPa.s, respectively, the interfacial tension of DIW/oil and nanofluid/oil systems at 25°C are 27.35 mN/m and 15.9 mN/m, respectively. The effective viscosities of sample fluids are found to decrease significantly with increasing fluid temperature. The slightly low rate of decreasing viscosity of nanofluid with temperature compared to mineral oil could be due to nanoparticles clustering, and interaction potential which can mollify the effect of temperature for nanofluid. Figure 2 also shows that nanofluid exhibits significantly smaller interfacial tension in mineral oil compared to that of base fluid. In contrast to deionized water, the measured data for interfacial tension of nanofluid show nearly linear trend of decreasing with increasing temperature. The results clearly demonstrate that the interfacial tensions of this TiO_2 (15 nm)/DIW-based nanofluid are significantly smaller and decrease more rapidly with temperature than those of the base fluid. The reason is that nanoparticles can easily experience Brownian motion and interact with the liquid molecules resulting to a reduced cohesive energy at the interface. Moreover, an elevated temperature intensifies the Brownian motion and it is known that the lower the cohesive energy the smaller the surface or interfacial tension. Furthermore, nanoparticles can be adsorbed at an interface e.g. liquid-liquid and function in similar ways to surfactants to reduce the surface tension or interfacial tension (Binks 2002).

3.2 Droplet formation

Although several studies (Song et al. 2006; Xu et al. 2006; Garstecki et al. 2006) discussed the droplet formation process at T-junction, it will be briefed in this subsection for easy understanding by non-microfluidic researchers such as those working on nanofluids.

Similar to the mechanism of the interfacial tension measurement i.e. pedant drop method, the droplet formation process in T-junction holds the same concept. During the droplet formation, the interfacial tension between the two phases (i.e. carrier fluid and aqueous fluid) is large enough to hold the droplet from detachment. At the same time, the extruded aqueous phase volume grows as the flow proceeds which means that the effective drag force increases as the droplet grows. When the droplet growth reaches a stage whereby the drag force is large enough to overcome the interfacial tension force, the droplet will be detached and carried away downstream. Thus, the force balance between the shear force and the interfacial tension force determine the droplet size formed inside the microchannel. Recorded images shown in Fig. 3 depict the droplet formation process of DI water at the T-junction. At the initial stage of droplet formation, the aqueous phase extrudes into the main channel (channel for carrier fluid) and forms a half disk like extrusion as shown in Fig. 3a. As the flows proceed the extruded aqueous phase starts to grow and gains more volume. Meanwhile, the continuous flow of carrier fluid in the main stream deforms the extruded aqueous phase. Figure 3b illustrates the moment right before the detachment of the droplet and form into a droplet. The characteristic necking was clearly observed in our experiments as shown in Fig. 3b. The necking helps to connect the droplet between the aqueous phase inlets. Figure 3b also represents unconfined breakup of droplet which is expected because the width of the carrier channel is much larger than that of the injection channel of the T-junction devices used in this study. This unconfined breakup confirms that droplet size is primarily controlled by local shear stress (Christopher and Anna SL 2007). A newly formed droplet whose shape is not yet steady is depicted in Fig. 3c.

3.3 Effect of channel depth

The size of the droplet formed in a T-junction also depends on the dimensions of the devices (Xu et al. 2006). The effect of channel depth on the droplet formation process is investigated by using two T-junction devices of different depths (300 μm and 30 μm) and keeping the flow rate ratio and average flow velocity constant. Figure 4 depicts the normalized (by their nominal values at 25°C) droplet sizes for both channel depths as a function of temperature. At 25°C, the droplet sizes of deionized water formed in the T-junctions of 300 μm and 30 μm channel depths are found to be 334 μm and 85 μm, respectively. For the experiments with T-junction device of 300 μm channel depth, the flow rates of aqueous fluids (DI water) and the carrier fluid (oil) were 60 μl/h and 120 μl/h, respectively. It is found that the overall droplet size increased by 12% when the heater temperature increased from 25°C to 39°C (see Fig. 4). During experiment with T-junction device of 30 μm channel depth, the same flow rate ratio of 1:2 (i.e. DIW flow rate/oil flow rate) was used. However, as the channel depths of this device is ten times smaller than the other device, both flow rates are kept ten times smaller which are 6 μl/hr and 12 μl/hr for aqueous fluid and carrier fluid, respectively. The lower flow rates make sure that the average flow velocity, which is proportional to the flow rate over the channel depth, remains same for both channel depths. Figure 4 also demonstrates that the increase of droplet size with temperature is substantially higher for smaller channel depth than that of the larger depth channel. For example, for an increase in temperature of about 14°C, the overall droplet size increase for this T-junction device (30 μm depth) was observed to be about 53% whereas increase in droplet size for larger channel depth (i.e. 300 μm) was only 12%. This is because the heating effect becomes more significant for the smaller channel

depth compared to the larger one resulting in larger increase in droplet size with temperature. Due to the smaller cross sectional area, the thermal gradient around the T-junction of the smaller depth channel is larger compared to the larger depth channel. The effect of thermal gradient on droplet size will be discussed in the following section (i.e. 3.4).

3.4 Effects of temperature and dispersed nanoparticles on droplet size

Fixing all geometrical parameters as well as the flow rates, the control over droplet size can be achieved with precise control of the temperature at the T-junction. In addition, dispersion of nanoparticles in the base fluid can also influence its droplet formation and size manipulation. In order to investigate these effects, the droplets of DI water and nanofluids were produced at a T-junction microchannel of 30 μm depth at different temperatures and at constant flow rates 6 μl/h and 12 μl/h for the aqueous fluids (DI water and nanofluids) and the carrier fluid (oil), respectively. Figure 5 shows the recorded images for the effect of temperature on droplet size for deionized water. The images clearly demonstrate that with an increase in temperature the droplet size increases significantly. It can be seen from Fig. 6 that the overall increase of DI water droplet size is about 53% for an increase in temperature of only 14°C (i.e. from 25°C to 39°C). The heater generates a thermal gradient in the carrier fluid around the T-junction resulting in a lower viscosity and a reduced interfacial tension between aqueous fluid and carrier fluid. The increase of temperature results in a faster decrease in viscosity than the interfacial tension (see Fig. 2). The extended droplet detachment time leads to larger droplets compared to those formed without any thermal effect. In addition, the droplet diameter is proportional to the ratio between the interfacial tension and the dynamic viscosity (Nguyen et al. 2007; Taylor 1934). Therefore,

the size of formed droplet in a microchannel increases with increasing heater temperature as shown in Figs. 4-6.

Figure 6 also compares the droplet sizes of deionized water and TiO_2 (15 nm)/deionized water-based nanofluid at different temperatures. The droplet sizes for these aqueous fluids were found to increase nonlinearly with increasing temperature. It can be seen from Fig. 6 that the droplet sizes of nanofluids are smaller than that of the base fluid and the dependency on temperature is less significant compared to the base fluid. Interestingly, this is in contrast to the trend observed in our previous work (Murshed et al. 2008). This is mainly because of different dimensions of microchannels and different flow rates of fluids used in present study. Nevertheless, the formation of smaller droplets in this study for this nanofluid compared to its base fluid may indicate the different flow regimes experienced at the T-junction. The difference between droplet sizes for nanofluid and deionized water (Fig. 6) is due to the different viscosity and interfacial properties of nanofluids as compared to DI water. During flowing through microchannels at such small flow velocity the agglomeration and sedimentation of nanoparticles may take place (Wen and Ding 2006; Timofeeva et al. 2007), which may also affect the droplet formation process.

3.5 Effect of nanoparticle shape on size of nanofluid droplet

The effect of nanoparticle shape on the droplet formation at different temperatures are also studied by using two different shapes (spherical and cylindrical) of TiO_2 nanoparticles in deionized water and the results are presented in Fig. 7. The T-junction microdevice of 30 μm channel depth was used for these experiments. The droplet size of nanofluid containing cylindrical-shaped nanoparticles was found to decrease with increasing temperature. This is in contrast to the trend observed for deionized water and other nanofluid. The reason for

such decreasing trend of droplet size is unclear at this moment and requires further investigations. Figure 7 also shows that addition of cylindrical-shaped nanoparticles in deionized water results in much larger droplet size compared to the spherical-shaped nanoparticles. Besides changing interfacial tension of DI water, nanoparticles can introduce interfacial slip at the interface. Such interfacial slip reduces the shear and can allow the droplet to grow. Due to alignments of cylindrical-shaped nanoparticles their interfacial shear can be smaller leading to larger droplet size as compared to nanofluids with spherical-shaped nanoparticles. Since no study was reported in the literature regarding the droplet formation of nanofluids at microfluidic T-junction, no comparison of the present results can be made.

4 Conclusions

From this study on droplet formation and size manipulation of deionized water and deionized water-based nanofluids in heat-induced microfluidic T-junctions, the following conclusions can be drawn.

First, the droplet size of deionized water was found to increase with increasing the heater temperature. This demonstrates that heating with an integrated microheater at the T-junction can effectively control the droplet formation and size manipulation.

Second, nanofluids exhibit different characteristics in droplet formation and size control with the temperature as compared to deiniozed water. Dispersion of small volume fraction of nanoparticles can substantially change the droplet size of deionized water formed at a microfluidic T-junction. The addition of small volume fraction of nanoparticles in deionized water can significantly alter the droplet formation process and its dependence on temperature. Nanoparticle shape was also found to have influence on the droplet formation

and size control. Apart from changing interfacial tension of DI water, nanoparticles introduce interfacial slip at the interface and thus influence the droplet formation of nanofluids particularly for cylindrical-shaped annoparticles.

Third, the dimensions of microchannels such as channel depth can significantly influence the droplet formation process. The smaller the depth of the channel the larger the increase of droplet size with temperature. In order to elucidate the mechanisms for droplet formation of nanofluids in microfluidic devices, further studies need to be conducted.

Acknowledgements

The authors gratefully acknowledge the support from the Agency of Science, Technology and Research (A*STAR), Singapore (grant number SERC 052 101 0108 "Droplet-based micro/nanofluidics").

References

Binks BP (2002) Particles as surfactants– similarities and differences. Curr Opin Colloid Interface Sci 7:21-41

Burns MA, Johnson BN, Brahmasandra SN, Handique K, Webster JR, Krishnan M, Sammarco TS, Man PM, Jones D, Heldsinger D, Mastrangelo CH, Burke DT (1998) An integrated nanoliter DNA analysis device. Science 282:484-487

Christopher GF, Anna SL (2007) Microfluidic methods for generating continuous droplet streams. J Phys D: Appl Phys 40:R319-R336

Garstecki P, Fuerstman MJ, Stone HA, Whitesides GM (2006) Formation of droplets and bubbles in a microfluidics T-junction–scaling and mechanisms of break-up. Lab Chip 6:437-446

Guttenberg Z, Müller H, Habermüller H, Geisbauer A, Pipper J, Felbel J, Kielpinski M, Scriba J, Wixforth A (2005) Planar chip device for PCR and hybridization with surface acoustic wave pump. Lab Chip 5:308-317

He M, Edgar JS, Jeffries GDM, Lorenz RM, Shelby JP, Chiu DT (2005) Selective encapsulation of single cells and subcellular organelles into picoliter-and femtoliter-volume droplets. Anal Chem 77:1539-1544

Joanicot M, Ajdari A (2005) Droplet control for microfluidics. Science 309:887-888

Lee S, Choi SUS, Li S, Eastman JA (1999) Measuring thermal conductivity of fluids containing oxide nanoparticles. J Heat Transfer 121:280-289

Li CH, Peterson GP (2006) Experimental investigation of temperature and volume fraction variations on the effective thermal conductivity of nanoparticle suspensions (nanofluids). Appl Phys Lett 99:084314-1– 084314-8

Link DR, Anna SL, Weitz DA, Stone HA (2004) Geometrically mediated breakup of drops in microfluidic devices. Phys Rev Lett 92:054503-1–054503-4

Murshed SMS, Leong KC, Yang C (2005) Enhanced thermal conductivity of TiO_2-water based nanofluids. Int J Therm Sci 44:367-373

Murshed SMS, Tan SH**,** Nguyen NT (2008) Temperature dependence of interfacial properties and viscosity of nanofluids for droplet-based microfluidics. J Phys D: Appl Phys 41:085502-1– 085502-5

Murshed SMS, Leong KC, Yang C (2008a) Thermophysical and electrokinetic properties of nanofluids– a critical review. Appl Therm Eng (in press, doi:10.1016/j.applthermaleng.2008.01.005)

Nguyen N T., Lassemono S, Chollet F (2006) Optical detection for droplet size control in microfluidic droplet-based analysis systems. Sens Actuat B 117: 431-436

Nguyen NT, Ting TH, Yap YF, Wong TN, Chai JCK, Ong WL, Zhou JL, Tan SH, Yobas L (2007) Thermally mediated droplet formation in microchannels. Appl Phys Lett 91:084102-1–084102-3

Nie ZH, Seo MS, Xu SQ, Lewis PC, Mok M, Kumacheva E, Whitesides GM, Garstecki P, Stone HA (2008) Emulsification in a microfluidic flow-focusing device: effect of the viscosities of the liquids. Microfluid Nanofluid, doi: 10.1007/s10404-008-0271-y

Nisisako T, Torii T, Higuchi T (2002) Droplet formation in a microchannel network. Lab Chip 2:24-26

Ong WL, Hua JS, Zhang BL, Teo TY, Zhuo JL, Nguyen NT, Ranganathan R, Yobas L (2007) Experimental and computational analysis of droplet formation in a high-performance flow-focusing geometry. Sens Actuat A 138:203-212

Schröder V, Behrend O, Schubert H (1998) Effect of dynamic interfacial tension on the emulsification process using microporous, ceramic membranes. J Colloid Interface Sci 202**:**334-340

Song H, Chen DL, Ismagilov RF (2006) Reactions in droplets in microfluidic channels. Angew Chem Int Ed 45:7336-7356

Taylor GI (1934) The formation of emulsions in definable fields of flow. Proc R Soc Lond A 146**:**501-523

Thorsen T, Roberts RW, Amold FH, Quake SR (2001) Dynamic patterned formation in a vesicle-generating microfluidic device. Phys Rev Lett 86:4163-4166

Timofeeva EV, Gavrilov AN, McCloskey JM, Tolmachev YV, Sprunt S, Lopatina LM, Selinger JV (2007) Thermal conductivity and particle agglomeration in alumina nanofluids: experiment and theory. Phys Rev E 76:061203-1–061203-16

Ting TH, Yap YF, Nguyen NT, Wong TN, Chai JCK, Yobas L (2006) Thermally mediated breakup of drops in microchannels. Appl Phys Lett 89:2234101-1–234101-3

Van der Graaf S, Steegmans MLJ, Schroen CGPH, Van der Sman RGM, Boom RM (2006) Lattice Boltzmann simulations of droplets formation in a T-shaped microchannel. Langmuir 22:4144-4152

Wen D, Ding Y (2006) Natural convective heat transfer of suspensions of titanium dioxide nanoparticles (nanofluids). IEEE Trans Nanotechnology 5:220-227

Whitesides GM (2006) The origins and the future of microfluidics. Nature 442:368-373

Xu JH, Li SW, Tan J, Wang YJ, Luo GS (2006) Preparation of highly monodisperse droplet in a T-Junction microfluidics device. AIChE J 52:3005-3010

Xu JH, Li SW, Chen GG, Luo GS (2006) Formation of monodisperse microbubbles in a microfluidic device. AIChE J 52:2254-2259

Zheng B, Roach LS, Ismagilov RF (2003) Screening of protein crystallization conditions on a microfluidic chip using nanoliter-size droplets. J Am Chem Soc 125:11170-11171

Figure captions:

Fig. 1 Schematic concept of a T-junction with integrated microheater and temperature sensor

Fig. 2 Temperature-dependent viscosity and interfacial tension of the investigated fluids (Viscosities and interfacial tensions are normalized by their nominal values at 25°C. At 25°C, viscosities of mineral oil and nanofluid are 26.4 mPa.s and 0.93 mPa.s, respectively, the interfacial tension of DIW/oil and nanofluid/oil systems are 27.35 mN/m and 15.9 mN/m, respectively)

Fig. 3 Deionized water droplet formation at 30 μm channel depth T-junction (Water and oil flow rates are 6 μl/h and 12 μl/h, respectively): (a) forming; (b) before detachment; (c) droplet after detachment

Fig. 4 Effect of microchannels depths on DI water droplet size at a constant flow rate ratio (DI water/oil) of 1:2 and average flow velocity (Droplet diameters are normalized by their nominal values at 25°C. At 25°C, the droplet sizes formed in the T-junctions of 300 μm and 30 μm channel depths are 334 μm and 85 μm, respectively.)

Fig. 5 Variation of DI water droplet size at different temperatures at 30 μm depth microchannel (flow rates of 6 μl/h for water and 12 μl/h for oil): (a) 25°C; (b) 32°C, (c) 39°C

Fig. 6 Temperature dependence of droplets size of DI water and a nanofluid at 30 μm depth microchannel (Both DI water and nanofluid had same flow rates of 6 μl/h and oil flow rate was 12 μl/h)

Fig. 7 Effect of nanoparticle shape on temperature-dependent droplet size formed in T-junction of 30 μm channel depth at constant flow rates of 6 μl/h and 12 μl/h for nanofluids and oil, respectively

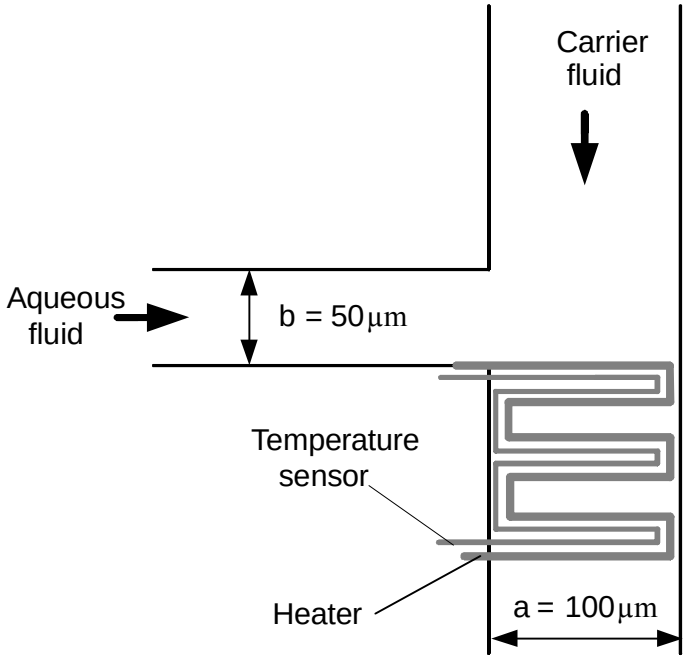

Fig. 1 Schematic concept of a T-junction with integrated microheater and temperature sensor

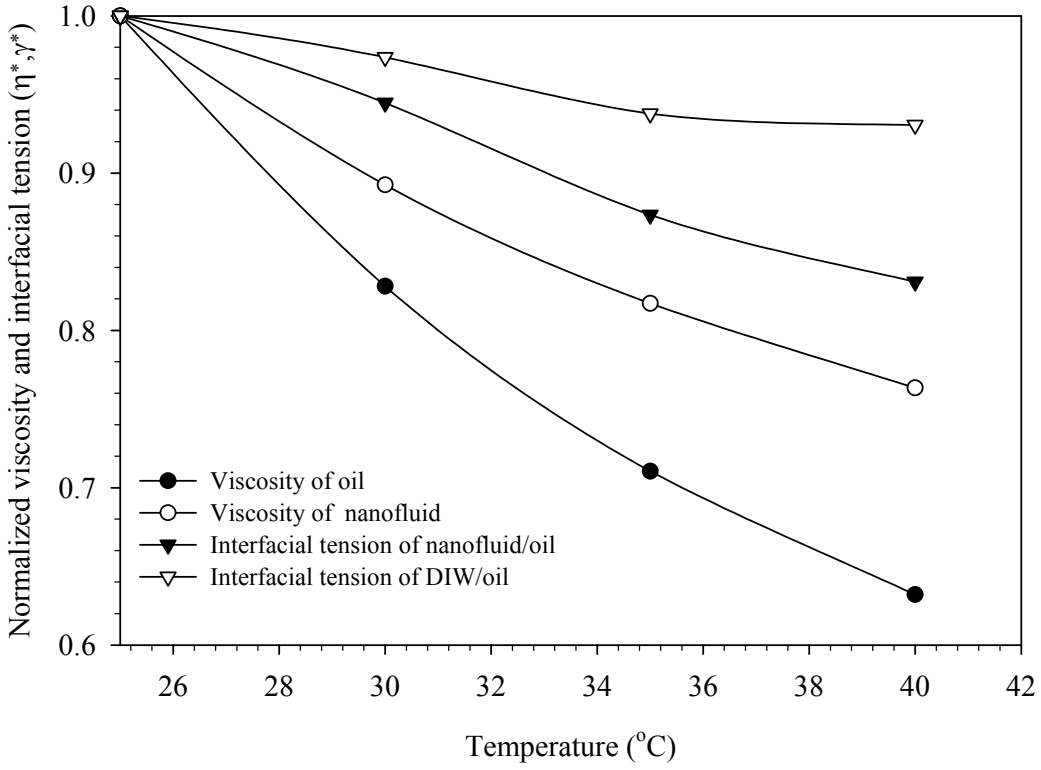

Fig. 2 Temperature-dependent viscosity and interfacial tension of the investigated fluids (Viscosities and interfacial tensions are normalized by their nominal values at 25°C. At 25°C, viscosities of mineral oil and nanofluid are 26.4 mPa.s and 0.93 mPa.s, respectively, the interfacial tension of DIW/oil and nanofluid/oil systems are 27.35 mN/m and 15.9 mN/m, respectively)

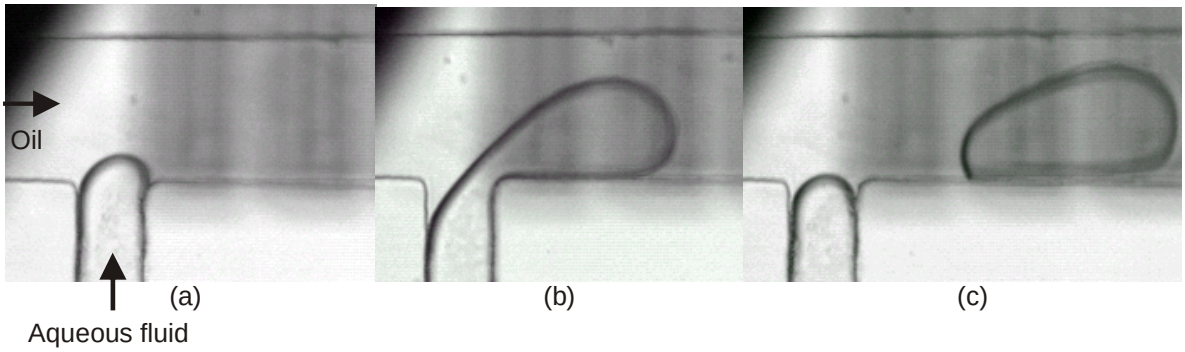

Fig. 3 Deionized water droplet formation at 30 μm channel depth T-junction (Water and oil flow rates are 6 μl/h and 12 μl/h, respectively): (a) forming; (b) before detachment; (c) droplet after detachment

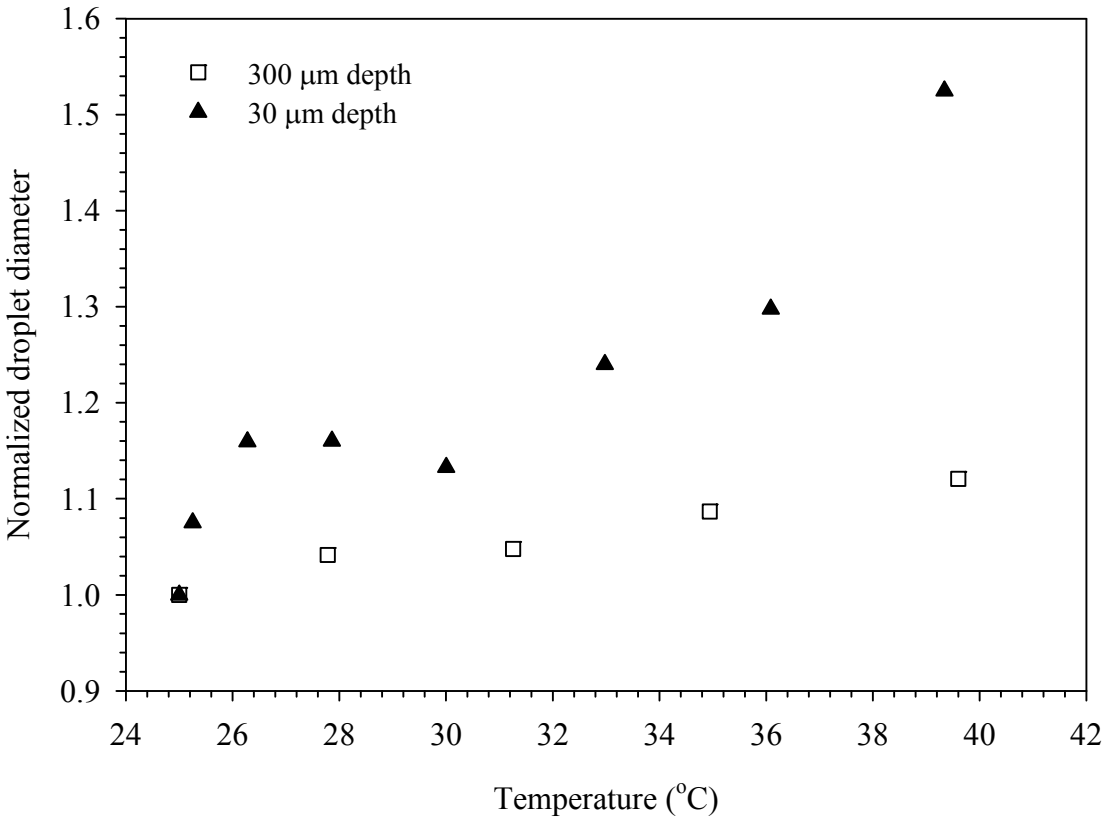

Fig. 4 Effect of microchannels depths on DI water droplet size at a constant flow rate ratio (DI water/oil) of 1:2 and average flow velocity (Droplet diameters are normalized by their nominal values at 25°C. At 25°C, the droplet sizes formed in the T-junctions of 300 μm and 30 μm channel depths are 334 μm and 85 μm, respectively.)

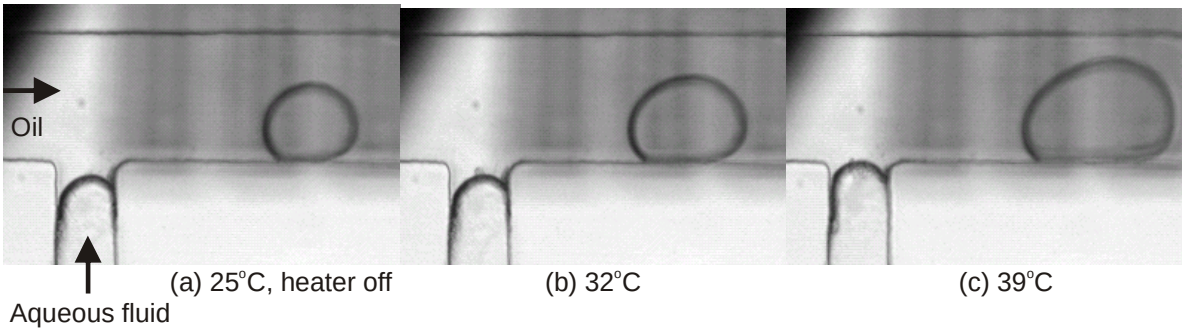

Fig. 5 Variation of DI water droplet size at different temperatures at 30 μm depth microchannel (flow rates of 6 μl/h for water and 12 μl/h for oil): (a) 25°C; (b) 32°C, (c) 39°C

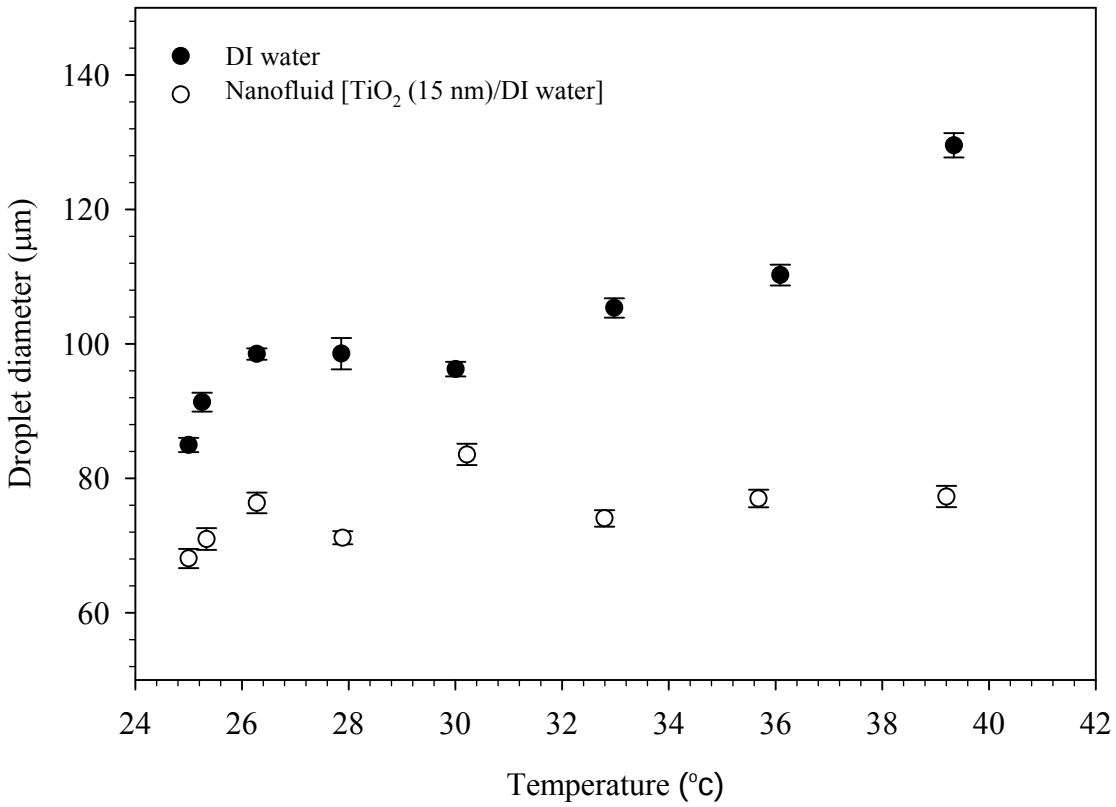

Fig. 6 Temperature dependence of droplets size of DI water and a nanofluid at 30 μm depth microchannel (Both DI water and nanofluid had same flow rates of 6 μl/h and oil flow rate was 12 μl/h)

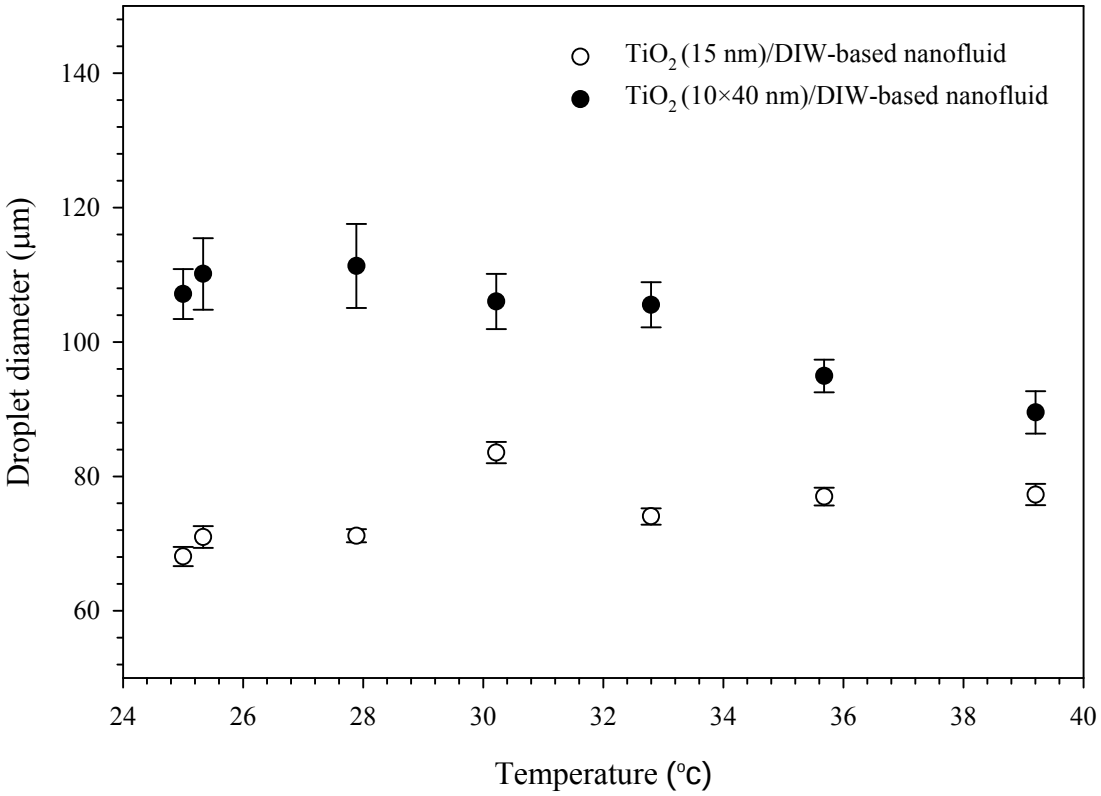

Fig. 7 Effect of nanoparticle shape on temperature-dependent droplet size formed in T-junction of 30 μm channel depth at constant flow rates of 6 μl/h and 12 μl/h for nanofluids and oil, respectively